

U.P. Suiinzhanova , A.U. Aldiyarov , K.I. Beisenov* 

Al-Farabi Kazakh National University, Kazakhstan, Almaty

*e-mail: khasen.007@gmail.com

STUDY OF GLASSY STATES OF CRYOCONDENSATES OF ORGANIC MOLECULES

Cryovacuum gas condensates, especially those prone to the formation of glassy states with their subsequent transformations, are ideal objects for studying the processes occurring in disordered amorphous solid-state systems. The fact that it is possible to precisely control the conditions of cryo-deposition, such as the condensation temperature and the rate of cryo-film formation, makes it possible to establish an unambiguous correlation between the properties of cryo-condensates and the specified conditions for their formation. Ultrastable glasses (predominantly from the vapor phase under optimal deposition conditions) are a unique class of materials with low enthalpies and high kinetic stability. These highly stable and dense glasses have unique physicochemical properties, such as high thermal stability, improved mechanical properties, or anomalous supercooled transitions. At $T = 70$ K, the transition from the amorphous glassy state (GS) to the liquid-solid cooled phase (SCL) occurs, after which its crystallization in the temperature range of 75-78 K passes into the plastic crystalline state (PC)-a cubic volume-centered structure with a directionally unregulated rotating subsystem. At $T = 78-80$ K, the transformation of the plastic crystal into a monoclinic crystal (MC) begins, which ends at $T = 83$ K.

Key words: ultrastable glasses, organic glasses, metallic glasses, Freon, crystallization, cryovacuum condensates.

Ұ.П. Сүйінжанова, А.У. Алдияров, Х.И. Бейсенов*

Әл-Фараби атындағы Қазақ ұлттық университеті, Қазақстан, Алматы қ.

*email: khasen.007@gmail.com

Органикалық молекулалар криоконденсаттарының шыны күйлерін зерттеу

Криовакуумдық газ конденсаттар, әсіресе олардың кейінгі түрленуімен шыны күйлерінің түзілуіне бейім, ретсіз аморфты қатты дене жүйелерінде жүретін процестерді зерттеу үшін тамаша объектілер. Конденсация температурасы мен криоқабықша түзілу жылдамдығы сияқты крио тұндыру жағдайларын дәл бақылау мүмкіндігі криоконденсаттардың қасиеттері мен олардың түзілуінің берілген шарттары арасында бір мәнді корреляцияны орнатуға мүмкіндік береді. Ультратұрақты шыны – (оңтайлы тұндыру жағдайында негізінен бұл фазасынан алынған) төмен энтальпиялары және жоғары кинетикалық тұрақтылығы бар материалдардың бірегей класы. Бұл өте тұрақты және тығыз шынылардың жоғары термиялық тұрақтылығы, жақсартылған механикалық қасиеттері немесе қалыптан тыс өте салқындатылған ауысулар сияқты бірегей физикалық және химиялық қасиеттері бар. $T = 70$ К шамасында аморфты шыны тәрізді (АШ) күйден сұйық-қатты салқындатылған (СҚС) күйге өту жүреді, содан кейін оның 75-78 К температура диапазонында кристалдануы пластикалық-кристалды (КПК) күйге өтеді, бұл – бағытталған-реттелмейтін айналмалы ішкі жүйесі бар текше денеге бағытталған құрылым. $T = 78-80$ К кезінде пластикалық кристалдың моноклиникалық кристалға (МК) айналуы басталады, ол $T = 83$ К болғанда аяқталады.

Түйін сөздер: ультратұрақты шынылар, органикалық шынылар, металл шынылар, фреон, кристалдану, криовакуум конденсаттары.

У.П. Суюнжанова, А.У. Алдияров, Х.И. Бейсенов*

Казахский национальный университет имени аль-Фараби, Казахстан, г. Алматы

*e-mail: khasen.007@gmail.com

Исследование стеклообразных состояний криоконденсатов органических молекул

Криовакуумные газовые конденсаты, особенно склонные к образованию стеклообразных состояний с последующими их превращениями, являются идеальными объектами для изучения

процессов, происходящих в неупорядоченных аморфных твердотельных системах. Возможность точного регулирования условий криоосаждения, таких как температура конденсации и скорость образования криопленки, позволяет установить однозначную корреляцию между свойствами криоконденсатов и заданными условиями их формирования. Ультростабильные стекла (преимущественно из паровой фазы при оптимальных условиях осаждения) представляют собой уникальный класс материалов с низкими энтальпиями и высокой кинетической стабильностью. Эти высокостабильные и плотные стекла обладают уникальными физико-химическими свойствами, такими, как высокая термическая стабильность, улучшенные механические свойства или аномальные переохлажденные переходы. При $T = 70$ К происходит переход из аморфного стеклообразного состояния (АС) в жидко-твердое охлажденное состояние (ЖТОС), после чего его кристаллизация в интервале температур 75-78 К переходит в пластично-кристаллическое состояние (ПК) – кубическую объемно-центрированную структуру с направленно-нерегулируемой вращающейся подсистемой. При $T = 78-80$ К начинается превращение пластического кристалла в моноклинный кристалл (МК), которое заканчивается при $T = 83$ К.

Ключевые слова: ультростабильные стекла, органические стекла, металлические стекла, фреон, кристаллизация, криовакуумные конденсаты.

Introduction

Since their discovery in 2007 by Mark Ediger and his group at the University of Wisconsin [1] at Madison, stable vapor-deposited glasses have become an important area of research in the glass community due to their remarkable properties that are facilitating new approaches to the investigation of some long-standing problems in glass science, such as the phenomenology of glass transitions and the existence or absence of ideal glass obscured by kinetic glass transitions observed in the laboratory. At the same time, vapor phase deposition offers a versatile method for the production of organic thin-film glasses with improved kinetic and thermodynamic stability, as well as an adapted molecular orientation, opening up new possibilities for increasing the efficiency and service life of organic optoelectronic devices. In a broad sense, glasses can be defined as non-equilibrium solids devoid of long-range order [2]. The lack of periodicity gives these materials exceptional properties. In particular, they can be made more uniform on a larger scale than crystals due to the absence of grain boundaries, and there is great flexibility in tuning their composition and properties without entering well-defined thermodynamic states. They demonstrate a reversible transition between glass and a supercooled liquid, called a glass transition. Therefore, a good understanding of the dynamic behavior of supercooled liquids is critical to an accurate understanding of glass formation. We refer the reader to several reviews devoted to the supercooled liquid state [3], here we briefly present some ideas that we consider important for further discussion.

Glass is usually made by cooling a liquid above the melting point of the material, bypassing

crystallization, to low temperature regions where the viscosity is high enough to consider the material to be solid on observable time scales [4]. In the glass state, molecular motion almost ceases, except for thermal vibrations. A similar statement can be formulated in terms of structural relaxation time τ (also called alpha relaxation), taking into account the Maxwell equation [5], which relates the relaxation time of a supercooled liquid and shear viscosity through $\tau = G_{\infty} \eta$, where G_{∞} is the shear modulus measured at high frequency. The relaxation time of the liquid is proportional to the viscosity and approximately corresponds to the same dependence on temperature, since the change in G_{∞} with temperature is much less abrupt than the change in viscosity. Therefore, like the viscosity, τ of the supercooled liquid increases sharply near the glass transition, although this dynamic change is not related to the structural change [6]. The relaxation time can be considered as a characteristic time associated with the restructuring of the system after it has undergone an external change and is out of equilibrium. This can also be related to the dissipation of spontaneous density fluctuations that arise in the liquid structure. Both characteristic times are related by the fluctuation-dissipation theorem. For example, when the temperature of a liquid drops by a small amount, its volume (or enthalpy) does not change immediately, but the process takes a certain time to reach equilibrium. This equilibration time (or relaxation time), which depends on temperature, determines the dynamics of such a change. The temperature at which the material relaxation time exceeds the standard laboratory time scales (conventionally chosen at about 100 s) is considered the standard glass transition temperature T_g (Fig. 1). This temperature marks the transition from a supercooled liquid to a glass state. The glass transition temperature can be determined in many

other alternative ways: for example, in calorimetric experiments, its value for a given substance is determined by the final heat capacity jump upon cooling from a liquid at a rate of -10 K/min (see Fig. 2) [8]. Throughout this review, by ordinary glass we mean glass cooled from a liquid at a rate of -10 deg/min, and its T_g is measured during cooling or subsequent heating at a rate of $+10$ deg/min. However, the temperature associated with atomic-molecular stopping depends on the thermal history of the material, that is, for example, on the rate of its cooling. The lower the cooling rate, the lower the glass transition temperature if crystallization can be avoided. In other words, glass can be made more stable (lower T_g on cooling) by simply reducing the cooling rate. Of course, in addition to the risk of crystallization, which is a hindrance to many families of glasses, there is a practical obstacle to this processing route, since, roughly speaking, glass production usually requires temperature deviations from the liquid state by tens/hundreds of degrees [7]. That is, cooling at a rate of 0.01 K/min per 100 K will require about 10 days. Further reduction by two orders of magnitude of the cooling rate to obtain glass with higher thermodynamic stability (lower T_g) will increase this number to 3 years.

The amount of increase in stability as the cooling rate decreases will ultimately depend on the brittleness of the supercooled liquid. Kinetic brittleness is a measure of the non-Arrhenius behavior of the change in viscosity (or relaxation time) of a supercooled liquid as it approaches the glass transition temperature. Strong liquids exhibit an Arrhenius temperature dependence, while brittle liquids are strongly non-Arrhenius [9]. The greater the deviation from Arrhenius, the greater the brittleness, as shown schematically in Fig. 1b. At this point, we introduce the potential energy landscape (PEL) paradigm that is so widely used to visualize and discuss the dynamic and thermodynamic behavior of glasses and viscous fluids. As shown in Fig. 3, the PEL of an ensemble of N particles is essentially a topographic projection ($3N + 1$) of the potential energy hypersurface of any glass-forming substance, although it is schematically projected over two dimensions for convenience. Even a small part of this energy diagram is a set of local minima and saddle points for thermal energies below kBT_m (where T_m is the melting point of the stable crystalline state when it exists [10]). When a liquid is supercooled, bypassing crystallization, to the glass transition temperature T_g , it becomes a glass, falling into one of many possible local minima or metastable states, depending on the subsequent thermal history.

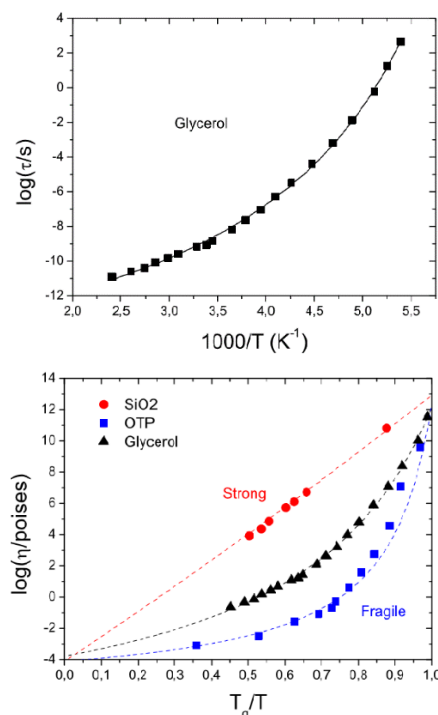


Figure 1 – Representation of the dynamics of typical glass-forming liquids: the logarithm of the structural (alpha) relaxation time of glycerol as a function of $1000/T$, showing an exponential increase in the relaxation dynamics with decreasing temperature, and the logarithm of the dependence of viscosity on the normalized reciprocal temperature for materials with different brittleness. Tough materials such as silica follow the Arrhenius expression, while brittle glass formers such as o-terphenyl follow the super-Arrhenius expression. Data obtained from [8]

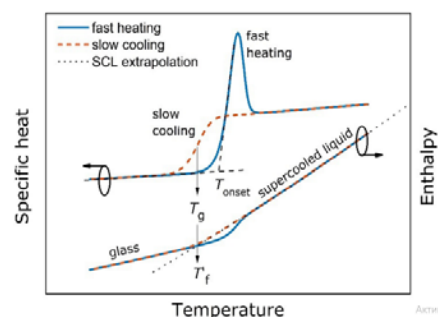


Figure 2 – Representation of a typical glass transition specific heat curve during cooling (red dotted line) and subsequent heating at a higher rate than during the previous cooling (blue line). The onset of the glass transition peak on heating corresponds to the initial temperature (T_{on}). Integrating the specific heat trace gives the enthalpy curve. The fictitious temperature limit can be calculated as the intersection of the enthalpy curve and the extrapolation of the enthalpy line of the supercooled liquid.

Many authors have speculated about the possible existence of an "ideal glass", which should correspond to the best and most stable glass possible, associated with the smallest relative minimum. This ideal glass would have to have zero configurational entropy, equal to the entropy of crystals, and was associated with the possible existence of an underlying thermodynamic glass transition, most likely of the second kind, occurring at the so-called Kauzmann temperature T_K . Interestingly, several experiments in the last decade have addressed this issue more directly, attempting to penetrate very deeply into the energy landscape, approaching the ideal glass state, as shown in Fig. 3. The recent emergence of highly stable glasses has opened up new possibilities. an attractive and timely window for investigating these issues in the real world, not speculative way. From the point of view of PEL, kinetic stability can be considered as the height of the barriers that must be overcome in order to reach another, more balanced, metastable state. Therefore, thermodynamic stability is represented by a deep position in PEL. The lower the T_f value, the higher the stability of the glass, or in other words, the lower the position of the glass in the PEL [11].

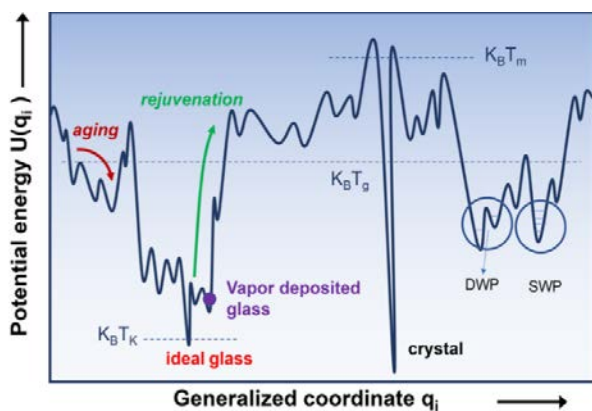


Figure 3 – Schematic potential energy landscape (PEL) for supercooled liquids and glasses, including a hypothetical absolute minimum for glass state. An ideal glass will be obtained after an infinitely long holding at the Kauzmann temperature T_K .

Double-well (DWP) and single-well (SWP) potentials are also offered (see Section 4 for a detailed discussion). Glass can evolve through aging, exploring lower energy states, or through rejuvenation, moving to higher energy states. Ultrastable vapor-deposited glass can achieve low-energy states close to ideal glass.

Materials

Organic glasses. Most of the work on ultrastable glasses is related to molecular glasses. Since the first measurements in 2007 [12] with 1,3-bis-(1-naphthyl)-5-(2-naphthyl)benzene (TNB) ($T_g = 347$ K) and indomethacin (IMC) ($T_g = 315$ K), over 45 different organic molecules, ranging from small molecules such as toluene and ethylbenzene to pharmaceuticals such as IMC and TNB, and more recently to organic semiconductors such as TPD, NPD, and TPBi. Have shown their ability to form highly stable glasses when grown by physical vapor deposition under the right processing conditions. As a general rule, vapor-deposited organic glasses show a significant increase in T_{on} compared to conventional glass obtained by cooling a liquid at a rate of -10 K/min. T_{on} ranges approximately from 2 to 10% depending on the molecular system and growth conditions. The two most significant external parameters affecting the kinetic and thermodynamic stability of organic glasses deposited from the vapor phase are the substrate temperature during growth from vapor, T_{sub} , and the growth rate, g .

This deposition method can produce highly stable glasses at lower deposition temperatures compared to standard physical vapor deposition. Other external variables such as electric/magnetic fields or light during thin film growth may have some influence on the formation of stable glasses depending on the nature of the organic molecule. For example, organic molecules with large intrinsic electric dipole moments can be orientationally tuned by strong external electric fields while maintaining high thermodynamic stability. The presence of magnetic fields during deposition can also play a role in molecules containing magnetic atoms. Alternatively, illumination of the substrate during growth can affect the formation of semiconductor molecules with homo-lumo levels below the energy of the incident light [13]. Eventually, as T_{sub} decreases further, the orientation of the molecule becomes flatter (parallel to the substrate), see Fig. 5. These observations have been experimentally determined using variable angle spectroscopic ellipsometry, X-ray diffraction, infrared/UV spectroscopy, or absorption and confirmed by a number of simulations [14]. The extent to which molecular ordering and thermal stability are related is not well known, but several experiments indicate that the two properties are not correlated.

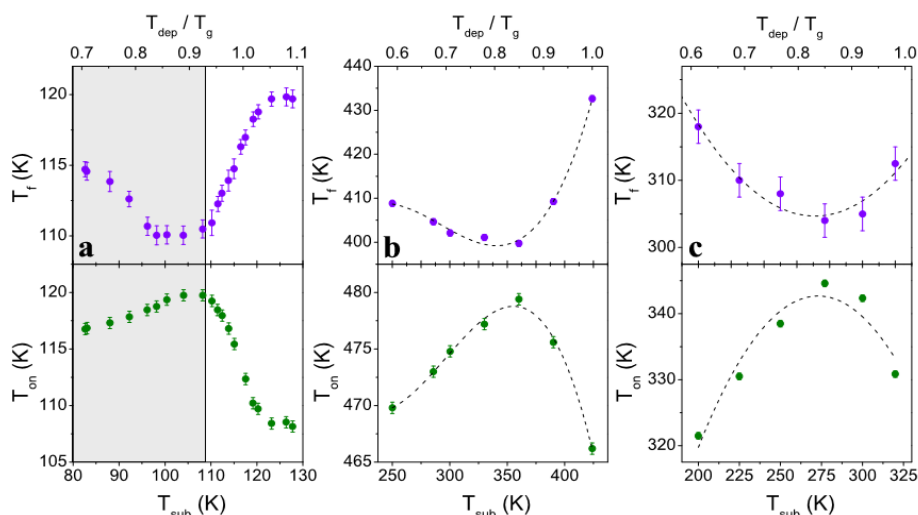


Figure 4 – Devitrification onset temperature (bottom) and fictitious temperature (top) of several organic thin films: Toluene; b Tris(4-carbazoyl-9-ylphenyl) amine (TCTA), c Celecoxib. The lines serve as a guide for the eyes. The devitrification was measured by quasiadiabatic membrane nanocalorimetry at heating rates on the order of 3×10^4 K/s for films of the same thickness.

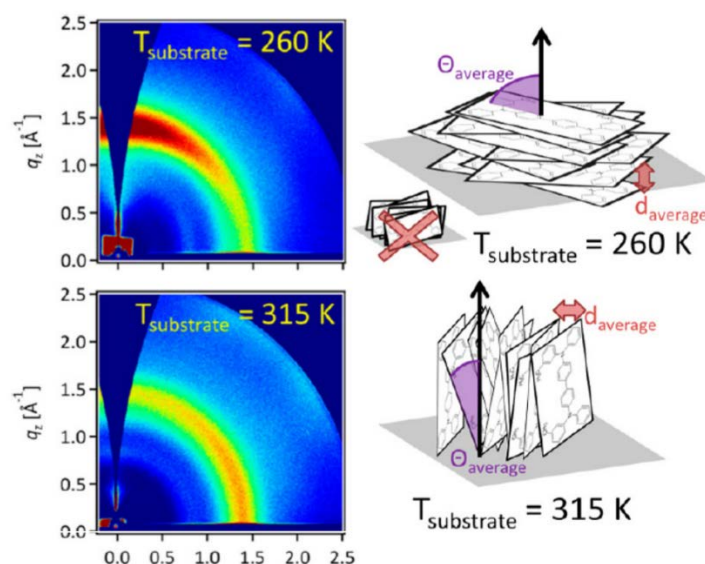


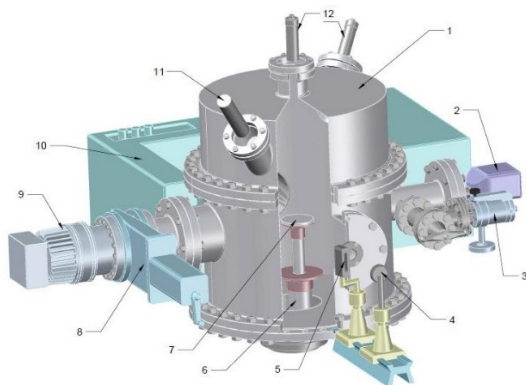
Figure 5 - (left) GIWAXS scattering patterns obtained from TPD glass vapors deposited at substrate temperatures of 260 K and 315 K. The intensity concentration observed along q_z and q_{xy} indicates anisotropic packing. These scattering patterns were obtained at an angle of incidence of 0.14° and reflect scattering from the entire thickness of the film. (Right) Diagram showing the microstructures of TPD glasses with the highest positive and negative order parameters in this study corresponding to the sample prepared at 260 K and 315 K. For illustrative purposes, the degree of order in the schemes is increased [15].

Experiment

Comprehensive studies were carried out on an experimental setup, which is a universal vacuum spectrophotometer, developed and created in the laboratory of cryophysics and cryotechnology of the Faculty of Physics and Technology. The technological parameters of the experimental setup make it possible to carry out measurements with an ultimate vacuum in the working chamber of the setup of 10^{-8} Torr, in the operating temperature range of

the cryosurface from 16 to 200 K, in the spectral range from 400 to 4200 cm^{-1} . The controlled thickness of the cryofilms was in the range from 0.25 to 25 μm . Figure 6 shows a scheme of a universal experimental setup, which was used to study the effect of polymorphic transformations in thin films of cryovacuum condensates of methane, methanol, ethanol, and freon 134a on optical characteristics, and also to determine the temperature limits for the existence of their structural-phase states. The universal experimental setup is a vacuum cryogenic

spectrophotometer, the main part of which is a vacuum chamber (1), 450 mm in diameter and height. The creation of vacuum in the chamber is carried out by a turbomolecular pump (9) Turbo-V-301, through a vacuum lock (8). The maximum vacuum value in the chamber reached $P = 10^{-8}$ Torr. Pressure measurement was carried out using a pressure transducer FRG-700 (2) connected to an AGC-100 controller. The main element of the chamber is a cryosurface (7) with a diameter of 60 mm and a height of 5 mm, which is installed on the upper flange of the microcryogenic machine (6) Gifford-McMahon. To ensure a sufficiently high thermal conductivity, the cryosurface was made of copper, and its polished surface was coated with a layer of silver to increase the reflectivity. Temperature measurements on the cryosurface were carried out with a thermal converter and a Lake Shore 325 controller. The mass of the injected gas condensed on the substrate was determined using a gas leak from a calibrated volume. The growth rate and film thickness were measured with a two-beam laser interferometer (wavelength 630 nm) using a P25a-SS-0-100 photomultiplier (12). The vibrational spectra of the resulting film were measured using an IKS-29 (10) IR spectrometer in the frequency range 400–4200 cm^{-1} .



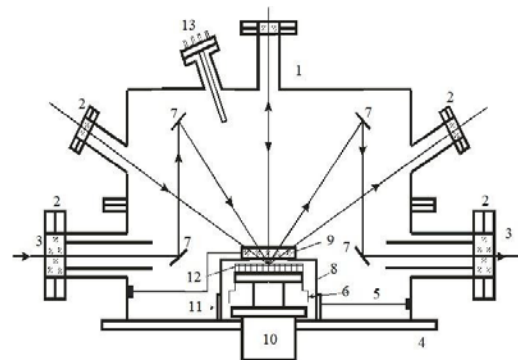
- 1 – vacuum chamber; 2 – pressure transducer;
 3 – system of the studied gas; 4 – mirror reflector;
 5 – IR source radiation; 6 – microcryogenic machine;
 7 – cryosurface; 8 – vacuum lock,
 9 – turbomolecular pump; 10 – IR-spectrometer;
 11 – laser; 12 – photomultiplier

Figure 6 – Scheme of the experimental setup

Description of the main elements of the vacuum chamber in the form of a diagram is shown in Fig. 7.

Overall dimensions of the base of the vacuum chamber (4): diameter 450 mm and thickness 35 mm. Calibration and installation work was carried out by opening the cover of the vacuum chamber. Optical windows (3) located in the camera body (1) are

designed to input the radiation of a two-beam laser interferometer. The light guides (7) of the two-beam laser interferometer provide different angles of incidence of the beam on the cryosurface. The studies were carried out in the IR range. A refrigerator (10) is located in the center of the chamber. Cutting off the working surface (12) from uncontrolled precondensation processes is carried out using a protective plate of potassium bromide (9). Additional copper plates are placed on the upper low-temperature flange of the microcryogenic machine, which play the role of cryocondensation pumps (6). There are holes in the protective casing (8) that allow the cryo-pumping process to be carried out using a cylindrical valve (11) and a magnetic drive (5), this allows increasing the vacuum level in the chamber[16].



- 1 – camera body; 2 – technological windows;
 3 – optical window; 4 – base; 5 – magnetic drive;
 6 – cryocondensation pump; 7 – mirror light guides;
 8 – protective cover; 9 – plate; 10 – refrigerator;
 11 – cylindrical valve; 12 – cryosurface;
 13 – technological window

Figure 7 – Scheme of the vacuum chamber of the experimental setup

Overall dimensions of the base of the vacuum chamber (4): diameter 450 mm and thickness 35 mm. Calibration and installation work was carried out by opening the cover of the vacuum chamber. Optical windows (3) located in the camera body (1) are designed to input the radiation of a two-beam laser interferometer. The light guides (7) of the two-beam laser interferometer provide different angles of incidence of the beam on the cryosurface. The studies were carried out in the IR range. A refrigerator (10) is located in the center of the chamber. Cutting off the working surface (12) from uncontrolled precondensation processes is carried out using a protective plate of potassium bromide (9). Additional copper plates are placed on the upper low-temperature flange of the microcryogenic machine, which play the role of cryocondensation pumps (6).

There are holes in the protective casing (8) that allow the cryo-pumping process to be carried out using a cylindrical valve (11) and a magnetic drive (5), this allows increasing the vacuum level in the chamber [16].

Results and Discussion

The transformation of the vibrational spectra as the temperature changes, we can conclude that the cooling of the samples condensed at high temperatures also leads to a sharp change in the position and shape of the absorption bands corresponding to the characteristic frequencies of the methanol molecule. This fact especially clearly demonstrates the change in the shape and position of the band of libration oscillations. In this regard, we measured the thermogram of the cooling of the sample condensed at $T = 132$ K and then cooled to $T = 16$ K. The value $\nu = 715$ cm⁻¹ was chosen as the observation frequency. These data are shown below in Fig. 8. The right inset of the figure shows the spectra in the vicinity of this frequency, corresponding to the initial temperature $T = 132$ K and the final value $T = 16$ K.

As can be seen from Fig. 8, lowering the temperature of the sample leads to significant changes in the absorption spectrum. In this case, judging by the thermogram, these changes are carried out monotonically, however, at $T = 60$ K, a clear break is observed, which may indicate that at this temperature, a transition occurs between different states of the methanol cryofilm. allows us to conclude that a first-order phase transition may exist in this temperature range. The totality of the data obtained allows us to assume that in the studied temperature range there are several structural states of methanol and the corresponding structural transitions. In this case, the fact that we observed that changes in the vibrational spectra are observed with decreasing temperature allows us to conclude that a first-order phase transition may exist in this temperature range.

The left figure shows the change in reflectance at a wavelength of 406 nm for two angles of incidence of laser radiation (1,2) in comparison with the data of the IR thermogram (3) during heating of the methanol cryofilm. The right figure is a detailed fragment of the change in reflectivity in the vicinity of the glass transition temperature $T_g = 103$ K [17].

The currently available data of various authors do not allow unambiguous confirmation of this assumption, although a number of studies indicate the unique properties of solid methanol. Thus, it was shown in that the surface structure of a methanol cryofilm undergoes changes from the deposition temperature $T = 20$ K up to the glass transition

temperature $T_g = 103$ K. The reason for this is an increase in the diffusion activity of methanol molecules on the surface of cryocondensates with increasing temperature. Besides, it is noted that in the temperature range from 103 K to 118 K, crystallization processes occur in a supercooled liquid. In this regard, it seems interesting to compare our results in the IR range (thermogram) in the specified temperature range with the data on the change in the surface reflectivity of the sample at the wavelength of the laser radiation of the interferometer. These data for two angles of incidence of radiation $\alpha = 45^\circ$ and $\alpha = 90^\circ$ are shown in Fig. 9. It is assumed that structural transformations in the methanol cryofilm will affect the reflectivity of the surface and, as a result, the signal of the interferometers that detect the laser beam reflected from the surface will change. As can be seen from the results shown in Fig. 9, the data of the IR spectrometer and lasers are in good agreement with each other, confirming the existence of structural features in the temperature range of 16–30 K, in the vicinity of a temperature of 70–80 K, and also in the temperature range of 100–120 K. On the right The insert in Fig. 9 shows in more detail the change in the signals of laser interferometers in the temperature range from 103 to 115 K, which corresponds to the area of existence of a supercooled liquid. A sharp change in the nature of the reflection of laser radiation from the surface of the methanol cryocondensate confirms our conclusion that the value of the glass transition temperature is located in the vicinity of the temperature $T_g = 103$ K. In addition, the presence of a break in the dynamics of laser interferometer signals at a temperature of 105 K may indicate the existence of structural transformations in the sample at $T = 105$ K and $T = 115$ K, which is consistent with the data of [18]. We would also like to note the fact that we discovered the unusual behavior of the sample in the process of crystallization of the supercooled liquid phase. Earlier, we noted that we determined the temperature range in which this process occurs. It is the temperature range, and not its specific value. The reason for our assessment becomes clear from the analysis of the data shown in Figure 10. As can be seen from Fig. 10, the process of crystallization of the supercooled liquid phase of methanol occurs in a highly nonmonotonic manner, which is especially pronounced in the temperature range from 114 to 120 K. This may indicate a multi-stage process crystallization, when the formation of the subsequent state of methanol is limited by the formation of its previous state. This means that intermediate metastable states can exist between the liquid and crystalline phases of methanol in this temperature range [19].

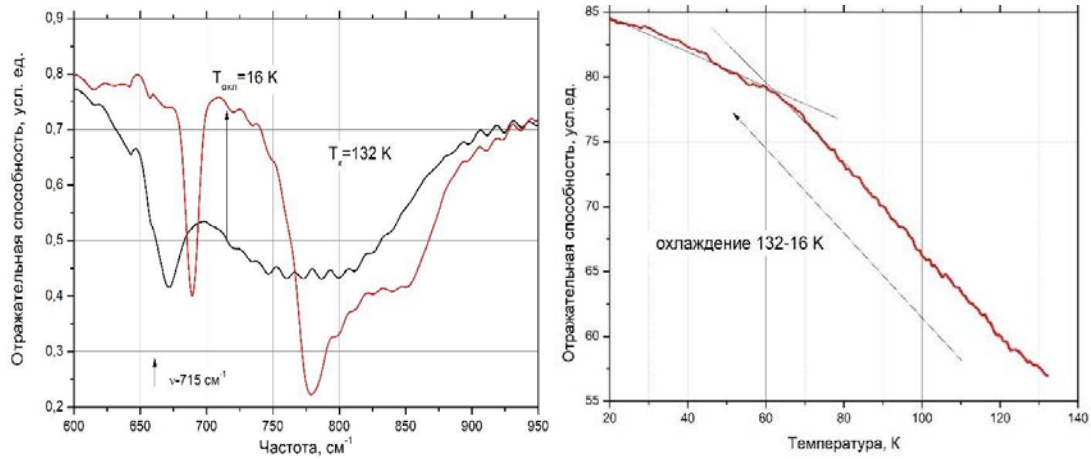


Figure 8 – Thermogram of cooling of a sample condensed at $T = 132$ K and cooled to $T = 16$ K, observation frequency $\nu = 715$ cm^{-1} (left), and comparison of the absorption spectra of a cryofilm condensed at $T_{dep} = 132$ K and cooled to $T_{cool} = 16$ K (right)

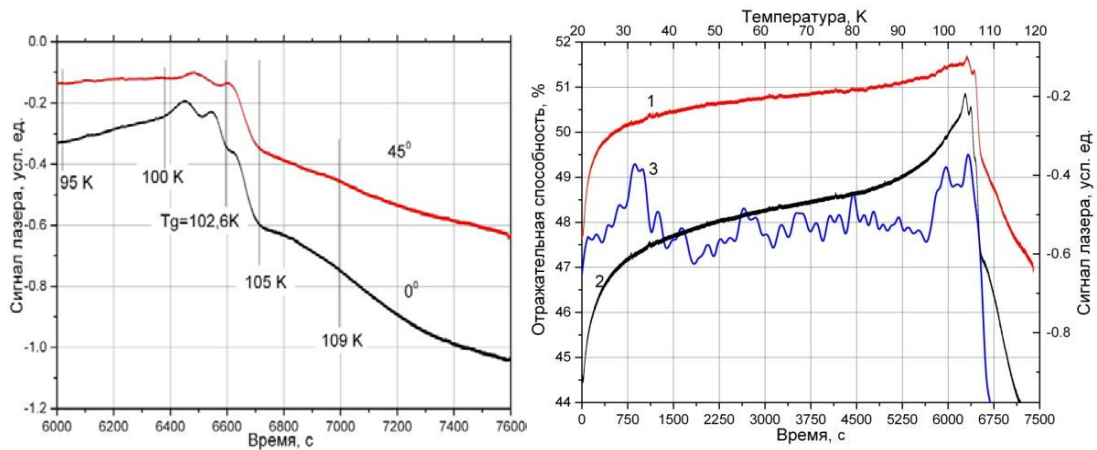
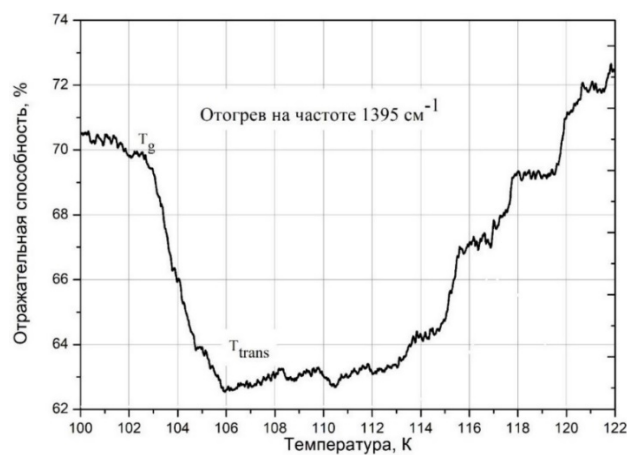


Figure 9 – Changes in the IR signal and laser in the vicinity of the glass transition temperature



T_g is glass transition temperature; T_{trans} is the transition temperature;

Figure 10 – Detailed representation of the thermogram of the heating of the methanol cryofilm in the temperature range of the existence of a supercooled liquid phase

Conclusions

At high densities and low enthalpies approaching "ideal glass", highly stable glasses exhibit unique liquefaction features such as the existence of a melt front in very thin films starting from high mobility regions located at surfaces/interfaces. Very thick (bulky) films have a glass transition resembling melting or crystallization by nucleation and growth. In this regard, there is still no understanding of the impact of stability in the mechanism of transformation. In addition, there are no detailed studies of the glass transition mechanism of ultrastable polymer and metallic glasses.

Based on the analysis of the results of measuring the IR spectra of methanol, the transition temperature from the glassy state (GS) to the state of supercooled liquid (SCL) was determined. In accordance with these results, the value of the glass transition temperature of methanol cryocondensates was determined to be $T_g = 102.6 \pm 0.2$ K, radiation $\lambda = 406$ nm. In addition, the temperature interval 103–118 K

for the existence of the SCL phase, as well as the interval 118–120 K, in which the SCL crystallization process is realized, was determined. Based on the data obtained, we determined the value of the glass transition temperature equal to $T_g = 102.6$ K, which is in agreement with the data of other authors. The range of temperatures for the existence of a supercooled liquid phase is determined in the range from 103 K to 118 K. We can assume that at a temperature of $T = 125$ K the sample is in a metastable state, and at a temperature of $T = 132$ K the cryofilm is in the α -phase. Cooling of cryocondensates formed at these temperatures leads to changes in the absorption spectra, which indicates structural transformations in them. In the general case, it can be said that at the same temperature, a sample of methanol cryocondensate can be in three different states, depending on the temperature history of its formation - direct condensation, heating from a low temperature state, or cooling from a higher condensation temperature.

References

- Swallen S.F., Kearns K.L., Mapes M.K. Organic glasses with exceptional thermodynamic and kinetic stability // *Science*. – 2007. – Vol. 315. – P. 353–356.
- Gonzalez L., Mo O., Yanez M. Density functional theory study on ethanol dimers and cyclic ethanol trimers // *The Journal of Chemical Physics*. – 2019. – Vol. 111. – P. 3855.
- Ediger M.D., De Pablo J., Yu L. Anisotropic vapor-deposited glasses: hybrid organic solids. // *Acc. Chem. Res.* – 2019. – Vol 52. – P. 407–414.
- Ediger M.D. Perspective: highly stable vapor – deposited glasses // *J.Chem.Phys.* – 2017. – Vol. 147. 210901.
- Bagchi K., Ediger M.D. Controlling structure and properties of vapor-deposited glasses of organic semiconductors: recent advances and challenges // *J. Phys. Chem. Lett.* – 2020. – Vol.11. – P. 6935-6945.
- Cavagna A. Supercooled liquids for pedestrians // *Phys. Rep.* – 2009. – Vol.476. – P.51-124.
- Maxwell J.C. IV. On the dynamical theory of gases // *Philos Trans R Soc London*. – 2009. – Vol.157. – P.49-88.
- Badrinarayanan P., Zheng W., Li Q., Simon S.L. The glass transition temperature versus the fictive temperature // *J Non Cryst Solids*. – 2007. – Vol. 353. – P. 2603-2612.
- Mauro N.A., Blodgett M., Johnsonetal M.L. A structural signature of liquid fragility // *Nat. Commun.* – 2014. – Vol. 5. – P.4616.
- Comez L., Masciovecchio C., Monaco G., Fioretto D. Progress in liquid and glass physics by Brillouin scattering spectroscopy // *Solid State Physics*. ed. by S. Sps. – 2012. – P.1-77.
- Yokoyama D., Sakaguchi A., Suzuki M., Adachi C. Enhancement of electrontransport by horizontal molecular orientation of oxadiazole planar molecules in organic amorphous films // *Appl Phys Lett*. – 2009. – Vol. 95. – P.243.
- Bagchi K., Jackson N.E., Gujraletal A. Origin of an isotropic molecular packing in vapor - deposited Alq3 glasses // *J. Phys. Chem. Lett.* – 2018. – Vol.10. – P.164–170.
- Moynihan C.T., Lee S.K., Tatsumisago M., Minami T. Estimation of activation energies for structural relaxation and viscous flow from DTA and DSC experiments // *Thermochim Acta*. – 2016. – P.280-281.
- Wolynes P.G. Spatiotemporal structures in aging and rejuvenating glasses // *Proc Natl Acad Sci USA*. – 2009. – Vol.106. – P.1353-1358.
- Goldstein M. Viscous liquids and the glass transition: a potential energy barrier picture // *J. Chem. Phys.* – 2003. – Vol.51. – P. 3728.
- Pogna E.A., Rodríguez-Tinoco C., Cerullo G. Probing equilibrium glass flow up to exapoise viscosities // *Proc Natl Acad Sci USA*. – 2015. – Vol.112. – P.2331–2336.
- Pablo G. Debenedetti, Supercooled and glassy water // *J. Phys. Condens.Matter*. – 2003. – Vol. 15 (45). – P. 1669.
- Pablo G., Frank H. Supercooled liquids and theglass transition *Nature* // *J. Phys. Condens.Matter*. – 2018. – Vol.410. – P. 259.

19 Chua Y., Tyliniski Z.M., Tatsumi S., Ediger M. D., Schick C. Glasstransition and stable glass formation of tetrachloromethane // J. Chem. Phys. – 2016. – Vol.144. – P.244503.

References

- 1 S.F. Swallen, K.L Kearns, & M.K. Mapes, *Science*, 315, 353–356 (2007).
- 2 L. Gonzalez, O. Mo, & M. Yanez, *The Journal of Chemical Physics*, 111, 3855 (2019).
- 3 M.D. Ediger, J. De Pablo, L. Yu, *Acc. Chem. Res*, 52, 407–414 (2019).
- 4 M.D. Ediger, *J.Chem.Phys*, 147, 210901 (2017).
- 5 K. Bagchi, M.D. Ediger, *J. Phys. Chem. Lett*, 11, 6935–6945 (2020).
- 6 A. Cavagna, *Phys. Rep*, 476, 51–124 (2020).
- 7 J.C. Maxwell, *Philos Trans R Soc London*, 157, 49–88 (2007).
- 8 P. Badrinarayanan, W. Zheng, Q. Li, S.L. Simon, *J Non Cryst Solids*, 353, 2603–2612 (2007).
- 9 N.A. Mauro, M.Blodgett, M.L. Johnsonetal, *Nat.Commun*, 5, 4616 (2014).
- 10 L. Comez, C. Masciovecchio, G. Monaco, D. Fioretto, In *Solid State Physics*. ed. by S. Sps, 1–77. (2012).
- 11 D. Yokoyama, A. Sakaguchi, M. Suzuki, C. Adachi, *Appl Phys Lett* , 95, 243303 (2009).
- 12 K. Bagchi, N.E. Jackson, A. Gujraletal, *J. Phys. Chem. Lett*, 10, 164–170 (2018).
- 13 C.T. Moynihan, S.K. Lee, M. Tatsumisago, T. Minami, *Thermochim Acta*, 280–281 (2016).
- 14 P.G. Wolynes, *Proc. Nat. Acad Sci USA*, 106, 1353-1358 (2009).
- 15 M. Goldstein, *J. Chem. Phys*, 51, 3728 (2003).
- 16 E.A. Pogna, G. Rodríguez-Tinoco, Cerullo G. et al., *Proc Natl Acad Sci USA*, 112, 2331-2336 (2015).
- 17 G. Pablo, *J. Phys. Condens.Matter*, 15 (45), 1669, (2003).
- 18 G. Pablo, *Nature*, 410, 259 (2001).
- 19 Y.Z. Chua, M. Tyliniski, S.M. Tatsumi, D. Ediger, C. Schick, *J. Chem. Phys*, 144, 244503 (2016).